

Tectonic Geomorphology of Wadi Wasit in Sinai Peninsula (Egypt)

Mr. Alaa Salah Othman Hassan

Department of Social Studies - Mansoura University

E-mail: alaasalah96@mans.edu.eg

Prof. Mohammed Mohammed Abdel All Ibrahim

Department of Social Studies - Mansoura University

TECTONIC GEOMORPHOLOGY OF WADI WASIT IN SINAI PENINSULA (EGYPT)

MR. ALAA SALAH OTHMAN HASSAN

Department of Social Studies -
Mansoura University

E-mail: alaasalah96@mans.edu.eg

PROF. MOHAMMED MOHAMMED ABDEL ALL IBRAHIM

Department of Social Studies -
Mansoura University

Abstract

Structural geomorphological landforms arise due to geological processes in tectonic regions. This study aims to identify the geomorphological landforms resulting from these processes in Wadi Wasit in the Sinai Peninsula in Egypt. The study depends on geological and topographic maps, aerial images, DEM (SRTM), fieldwork, and Global climate databases (POWER, ERA5). It used the GIS technique. The results showed that the surface rocks in the study area were deposited in the Upper Cretaceous, Paleocene, Eocene, Miocene, Pleistocene, and Holocene. The rocks consist of Limestone, Sandstone, Wadi deposits, Alluvial Hamadah deposits, and Conglomerate. It was affected by 41 faults and a concave fold. These tectonic processes formed geomorphological landforms in the study area, which are: Fault scarps, Cuesta scarps, Structural Basins, Faulted Wadies, and Gorges.

Key words: Tectonic Geomorphology, Faults, Wadi Wasit, Sinai Peninsula, GIS, Egypt.

1-Introduction

Tectonic geomorphology is concerned with structural geology, exploring the relationships between crustal movements, rates of surface processes, and the development of landforms. Bull (2007) put an emphasis on processes because tectonic geomorphology includes the effects of crustal deformation and the resulting

landscape. The forms of Earth and its history are used to learn about active tectonic structures and understand faults and folds (Różycka, Migoń, 2017).

The study of tectonic processes is useful in understanding the formation of geomorphological landforms in any region affected by these processes (Zovoili et al., 2004). This type of study gives more understanding of past tectonic events during geological times (Torab, 2022). The study area is located in the western central sector of the Sinai Peninsula, which is one of the most active areas due to the rupture of rocks by faults (Ball, 1916). So, this paper aims to understand the geological characteristics and tectonic geomorphological landforms of the study area.

Many studies have presented geomorphological interests in West Central Sinai, including geomorphological landforms, geomorphological mapping, sediment analysis, and flood hazards (e.g. Ismail, 2017; Abu Al-Yazid, 2016; Shelby, 2013; Qaqa, 2010; Hassan, 2007; Ghallab, 2006; Mashadi, 2005; Al-Nagger, 2003; Al-Rashidi, 1994; Al-Awadi, 1993). These studies did not provide any details about tectonic geomorphological landforms in Wadi Wasit. The main idea of the current study is the geomorphological landforms resulting from tectonic processes. This study used data integration methodology between geological and topographic maps, digital elevation model (SRTM), aerial images, GIS technique, and fieldwork.

2- Study area

The study area is located in the west-central sector of the Sinai Peninsula, between latitudes $29^{\circ} 10' 17''$ N and $29^{\circ} 18' 29''$ N and longitudes $33^{\circ} 11' 4.9''$ E and $32^{\circ} 54' 32''$ E. It has an area of 128 km²,

a length of 25.6 km, and maximum width of 8 km. The elevation varies between 800 m in the east and 0 m in the west close to the Gulf of Suez at sea level. The study area is located in the tectonic groove, east of the Gulf of Suez, between Wadi Ghrandal in the north and Wadi Thal in the south (Fig.1).

The study area is situated in the arid zone in the Sinai Peninsula, with hot summer and cold winter (Musaed, H. et al., 2022). Its maximum temperature is 38.7 °C in summer and the minimum temperature is

3.8 °C in winter. Wind speed rates range between 14.5 km\ h in June and 10.9 km/h in January. Relative humidity varies between 40.2 % in summer and 53.6 % in autumn. Evaporation rates range between 1.7 mm\ day in winter and 4.5 mm\ day in summer (Tab.1) (Fig.2).

Table 1: Climate variables data in the study area (1984 - 2020).

Climate variables	Max temperature (°C)	Min temperature (°C)	Temperature range (°C)	Wind speed (km/h)	Wind direction °	Precipitation (mm)	Relative humidity (%)	Evaporation (mm)
January	23.1	3.8	19.3	10.9	278.0	0.2	59.8	1.6
February	25.9	4.2	21.7	11.3	289.0	0.2	54.7	2.0
March	29.5	5.7	23.8	12.4	300.3	0.2	49.3	2.9
April	34.7	8.6	26.1	12.6	208.3	0.0	41.1	4.0
May	37.7	12.4	25.4	13.2	201.0	0.0	37.5	4.8
June	38.7	15.7	23.0	14.5	345.0	0.0	38.4	5.3
July	38.6	18.3	20.4	13.1	335.0	0.0	39.2	3.4
August	38.0	19.1	18.9	13.5	329.7	0.0	43.1	4.8
September	37.1	17.1	20.0	14.7	247.9	0.0	49.7	4.1
October	34.6	13.9	20.7	12.9	166.9	0.0	54.0	3.0
November	29.4	10.2	19.2	11.4	266.5	0.1	57.2	2.0
December	24.7	5.5	19.2	10.9	279.7	0.2	59.4	1.6
winter	24.5	4.5	20.1	11.0	282.2	0.2	57.9	1.7
Spring	34.0	8.9	25.1	12.7	236.5	0.1	42.6	3.0
Summer	38.4	17.7	20.8	13.7	336.6	0.0	40.2	4.5
Autumn	33.7	13.7	20.0	13.0	227.0	0.0	53.6	3.9
Annual rate	32.7	11.2	21.5	12.6	270.6	0.1	48.6	3.3

Data source: POWER and ERA5.

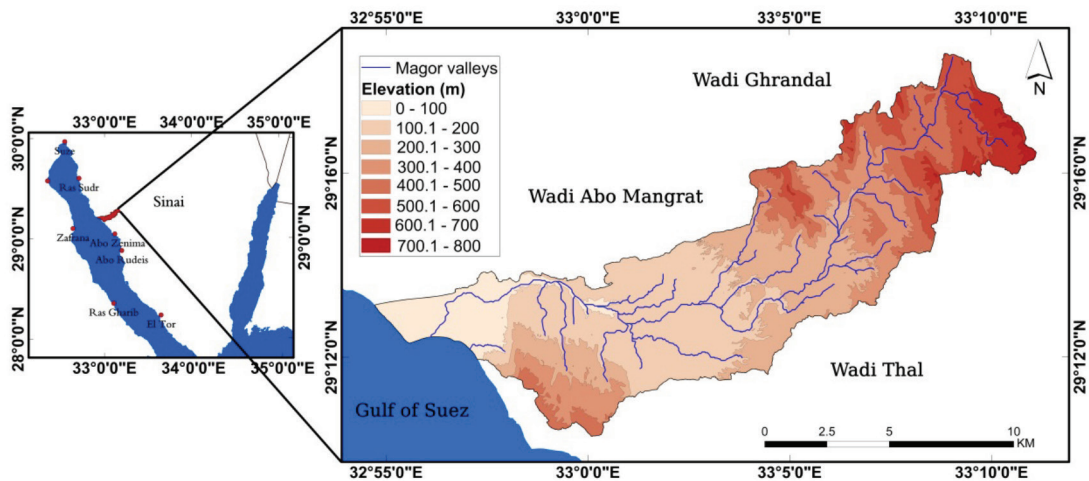


Fig. 1: Location map of the study area.

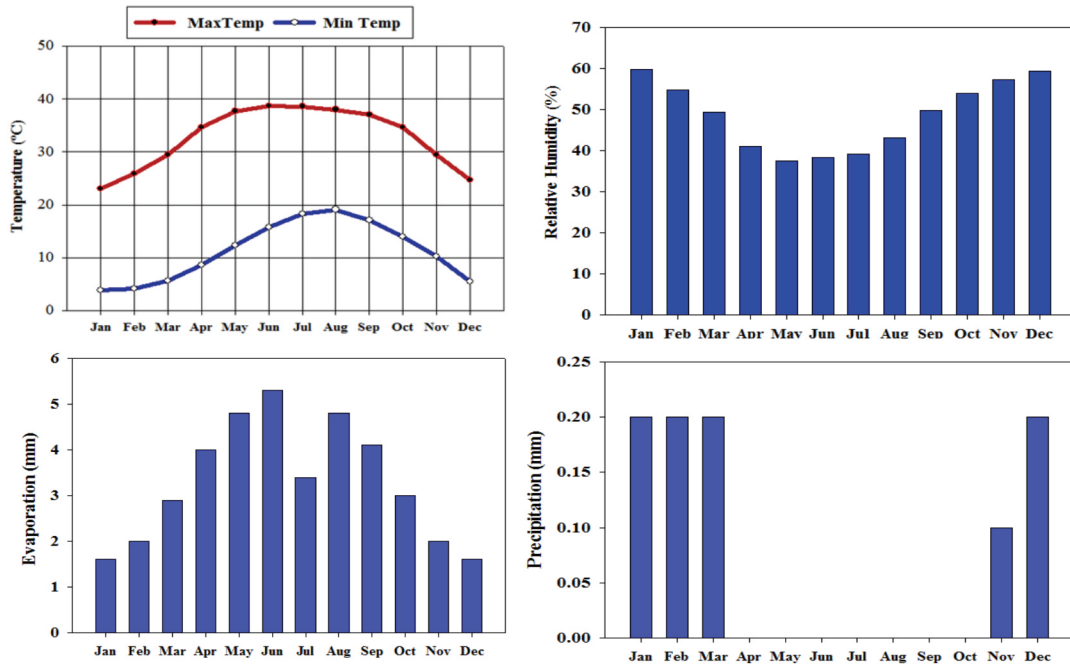


Fig. 2: Climatic conditions in the study area between 1984- 2020.

Data source: POWER and ERA5.

3- Materials and methods

The study depends on geological and topographic maps, a digital elevation model (SRTM), aerial images, global climate databases, and fieldwork. The data were processed and analyzed by using ArcGIS 10.5 (Fig. 3).

3.1- Geological analysis

The study depends on the geological map of Sinai, Arab Republic of Egypt (Sheet N.3, 1994, Scale 1:250000) to analyze geological structures, which are geological formations, faults, and folds. In addition to drawing a geological map of the study area.

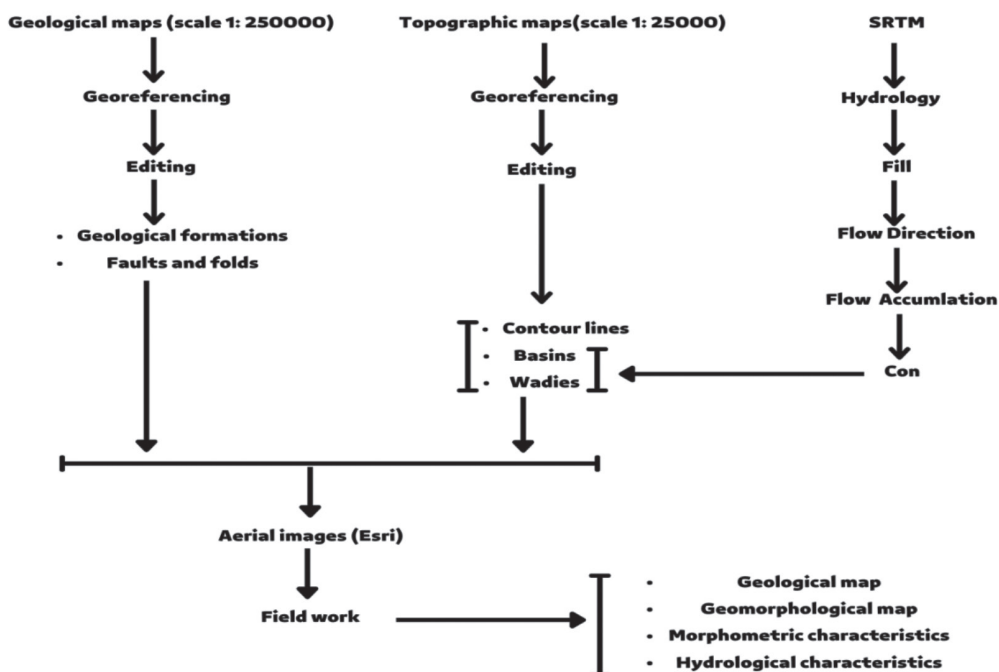


Fig. 3: The methodology of processing and analyzing data.

3.2- Climatic analysis

The study used global climate databases to get the Climate data, which are POWER and ERA5. Many past studies depend on these databases to get and analyze Climate data (e.g. Rockett, P., 2021; Deshmane, M et al., 2020; Chandler, W et al., 2015; Zhang, T et al., 2010; Puri, P., Puri, V., 2022; Sando, R. et al., 2022; Marelign, M. A. et al., 2020). The current study used POWER to download temperature data °C, wind speed (km/h), and relative humidity (%) (<https://power.larc.nasa.gov/data-access-viewer>).

It used ERA5 to download wind direction (°), precipitation (mm), and evaporation (mm) (<https://cds.climate.copernicus.eu/>).

The study depends on a model to calculate wind direction data by using (the u-component of wind and v-component of wind) indexes, which are found in the ERA5 database. The wind direction data was calculated by the following equation (<https://confluence.ecmwf.int/>):

$$\phi = \text{Mod} \left(180 + \frac{180}{\pi} \right) \times \text{atan2}(u, v); 360$$

The Climate data were processed and analyzed by (Model Builder) in ArcGIS 10.5 program (Fig. 4). In addition to setting up grid points data of the study area (Fig. 5).

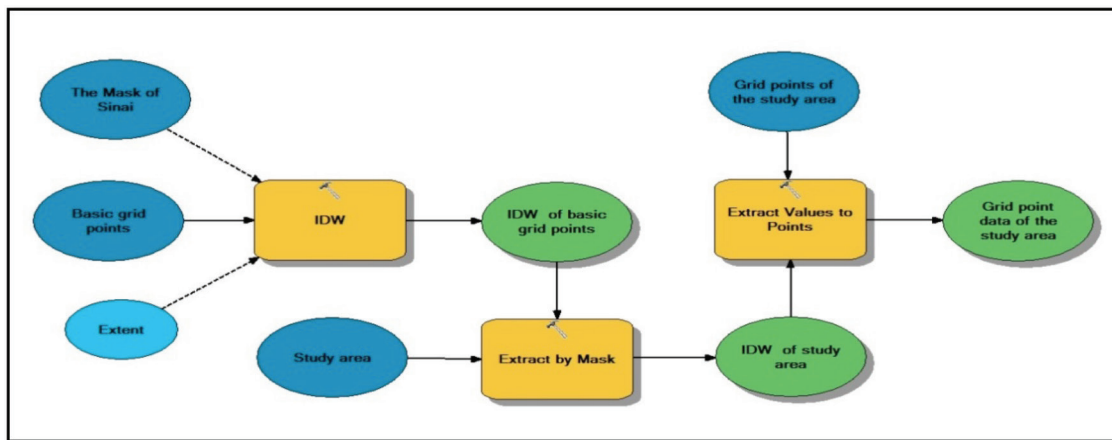


Fig. 4: The Model Builder of climate data processing and analysis.

Data source: POWER and ERA5.

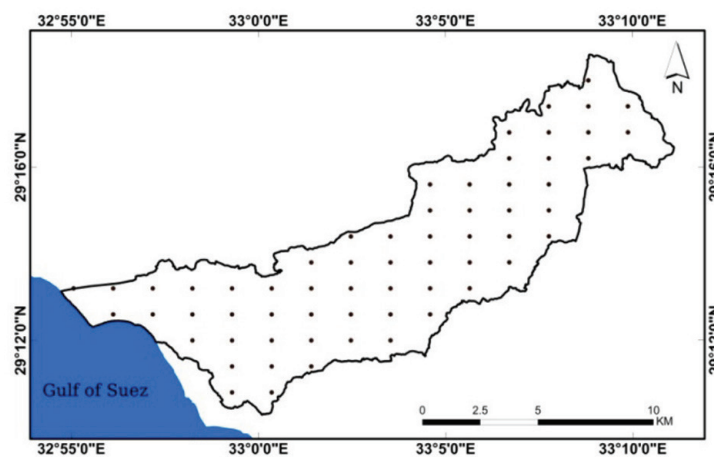


Fig. 5: Grid points data of the study area.

3.3- Topographical and hydrological analysis

The topographic maps (Scale 1:25000, Egyptian Military Survey Administration, 1998) with the digital elevation model (SRTM) were merged to get the elevation data. The SRTM DEM was used to determine the valley streams and their morphometric characteristics (Fig. 3).

3.4- Geomorphological analysis and fieldwork

The results of the former analyzes were used to study and draw the tectonic geomorphological landforms map in the study area. The study depends on SAS Planet 2019 program to download an aerial image with a resolution of $0,6 \times 0,6$ m. This image was used to draw the tectonic geomorphological landforms and calculate their morphometric characteristics. The fieldwork in Wadi Wasit helped to study the geological characteristics and measure some geomorphological landforms.

4- Results and Discussion

4.1- Geological settings

The study area consists of sedimentary rocks formed from the Upper Cretaceous time in the Paleozoic, up to the Holocene in the Cenozoic (Tab.2). The Upper Cretaceous formations consist of sedimentary chalky rocks (Fabricius,

2007) and are found on the top of shallow marine Jurassic carbonates due to sea level decline (Said, 1990). The Upper Cretaceous rocks in the study area consist of Jalala, Wata, Matallah, Duwwi, and Sudr formations (Fig.6).

Mesozoic formations were formed in the study area in Paleocene, Eocene, and Miocene. Paleocene is characterized by black shale (Smith et al., 2020). Its rocks are represented in the Esna Formation. It is surmounted by the formations of Egma, Darat (Fig.7: a), Samalut, Khabubah, Tanka (Fig.7: b), and Tayyabah in the Eocene (Fig.8: a). The Miocene rocks are represented in the Nukhl (Fig.8: b) and Rudays formations (Fig.8: c). The thickness of these rocks is 400 m in the Hammam Faraun block (Moustafa, Abdeen, 1992). Cenozoic deposits are Fanglerate, Alluvial Hamada, and Wadi deposits (Fig.9).

The morphology of the study area was affected by the number of 41 faults and the Thal-Wasit concave fold. This fold is located east of the Hammam Faraun block, with a length of 4 km (Fig.10).



Fig. 6: The upper Cretaceous formations in the study area.

Table 2: Rocks and geological formations in the study area.

Symbol	Time units		Formation	Lithology	Area (KM ²)	Percentage %
QW	Cenozoic	Holocene	Wadi deposits	Superficial sediments	8.3	6.5
Qh		Pleistocene	Alluvial Hamadah deposits		3.6	2.8
Qfg		Pleistocene	Fanglomerate		2.2	1.7
Total					14.1	11
Tmrd	Mesozoic	Lower Miocene	Rudays	Sandstone	33.3	25.9
Tmnk		Lower Miocene	Nukhl		5.6	4.4
Tety		Upper Eocene	Tayyabah		3.4	2.6
Tetk		Upper Eocene	Tanka	5.3	4.1	
Tekb		Middle Eocene	khabubah	4.7	3.7	
Tedr		Middle Eocene	Samalut	14.7	11.5	
Temn		Middle to Lower Eocene	Darat	11	8.5	
Telws		Lower Eocene	Egma	3.2	2.5	
Tpes		Lower Eocene-Paleocene	Esna	7.4	5.8	
Total					88.5	69
Ksd	Paleozoic	Cretaceous	Sudr	Limestone	5	3.9
Kdu			Duwwi		2.6	2
Kmt			Matallah		5.4	4.2
Kwt			Wata		12.6	9.9
Kjll			Jalalah		0.1	0.1
Total					25.6	20
The study area					128	100

Data source: Geological map of Sinai, 1994, Scale 1:250000.

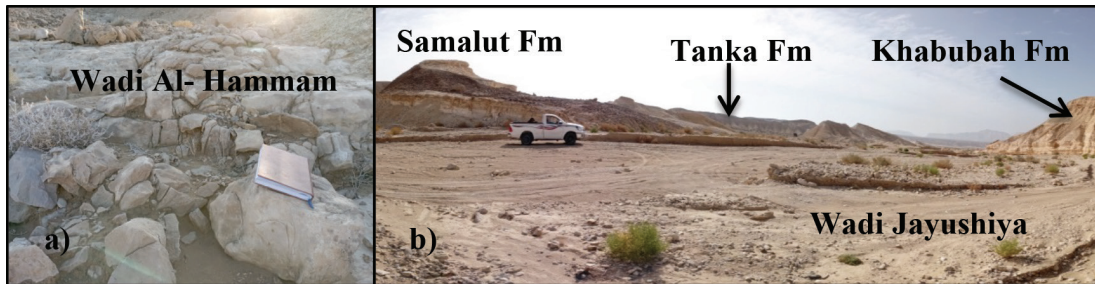


Fig. 7: The Eocene formations in the study area.

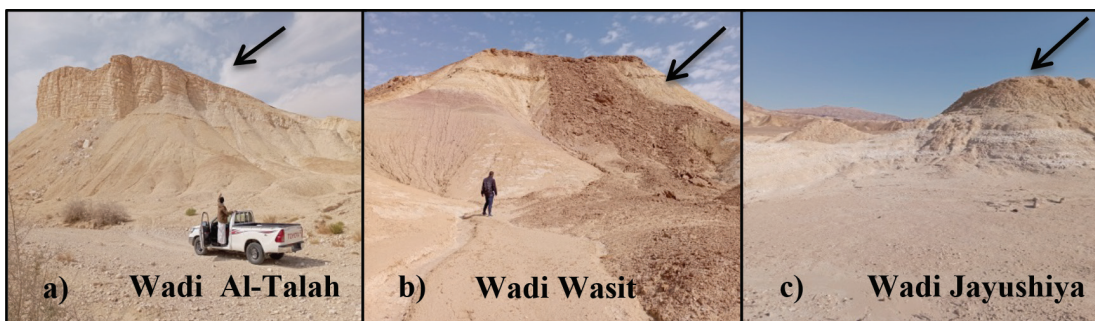


Fig. 8: The formations of Tayyabah, Nukhl and Rudays in the study area.



Fig. 9: The Cenozoic deposits in the study area.

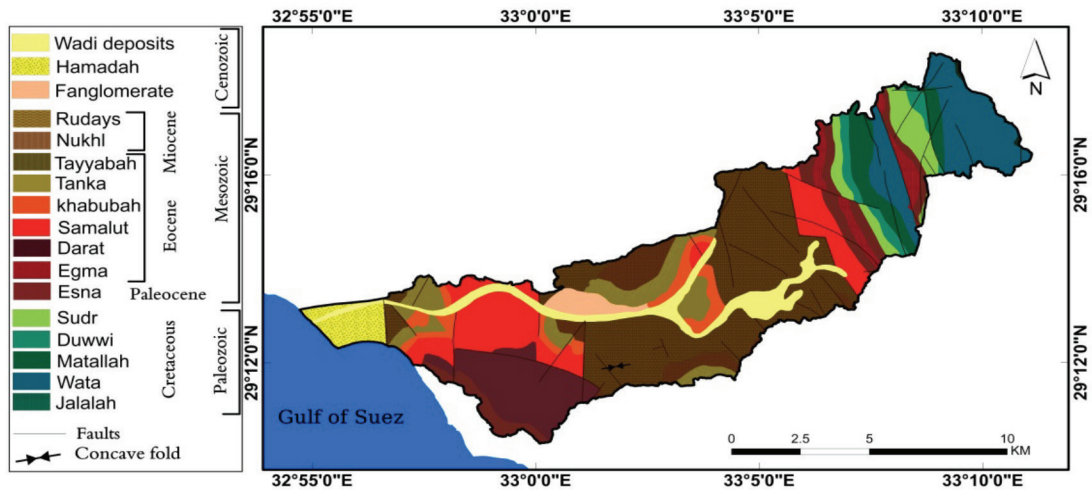


Fig. 10: Geological map of the study area.

Data source: Geological map of Sinai, 1994, Scale 1:250000.

4.2- Geomorphological landforms

The study area was affected by seven ground movements during its geological evolution, which resulted in a distortion in its surface

as well as the emergence of several geomorphological landforms

(Mustafa, 1996). The processes of these movements were faulting in most of its parts and folding in its lower sector (east of the Hammam Faraun block). These geomorphic features include escarpments, structural basins, faulted Wadies, and gorges (Fig.11).

4.2.1. Escarpments

Escarpments are slope surfaces resulting from faults, erosion, or the occurrence of undermining processes of the soft layers because of rocky difference (Al-Rifai et al., 1998). There are two types of these escarpments in the study area (Tab.3).

Fault Scarps

It is one of the structural geomorphological landforms related to faults (Stewart, Hancock, 1990). Among these scarps in the study area is the western scarp of Hammam Faraun. It consists of limestone rocks belonging to the Eocene. It was formed by the faulting of the

Hammam Faraun block. Furthermore, it has along of 4.1 km and a slope of 21° .

Its height ranges from 78 to 469 m (Fig.12).

Cuesta Scarps

The cuesta scarp creates due to the different rock formations and tilted structure. It consists of two opposite directions, which are dip-slopes and escarpment slopes (Torab, 2011). There are various cuesta scarps in the upper sector of the study area, for example, the center of

Al- Drairah Scarp. It is located in the central sector of Wadi Al-Darirah, with a length of 1.2 km. Its elevation ranges between 538–409 m, and its slope is 20.8° . It consists of cretaceous rocks (Wata formation). It is exposed to many geomorphological processes such as mechanical weathering, block separation, and rock fall. So it is an erosional scarp (Fig.13).

Table 3: Morphometric characteristics of the Escarpments in the study area.

Escarpments	Length (km)	Max Elevation (m)	Min Elevation (m)	Degree of slope °	Direction	Lithology
Faulty Scarps						
West of Hammam Faraun	4.1	469	78	21	North-south	Eocene limestone
Upper of Al-Drairah	4.8	636	493	26.2	North-south	Cretaceous limestone
Kreer	2.3	686	424	27	North-south	Paleocene limestone
Cuesta Scarps						
Southwest of Hammam Faraun	3.8	495	414	22.7	Northwest - southeast	Paleocene limestone and lava flow
Al-Drairah center	1.2	538	409	20.8	North - West	Cretaceous limestone
Abu Al-Lasf center	2	583	410	18.2	Northwest - south	Cretaceous limestone

Data source: Geological and topographic map, SRTM, and aerial images (Esri)

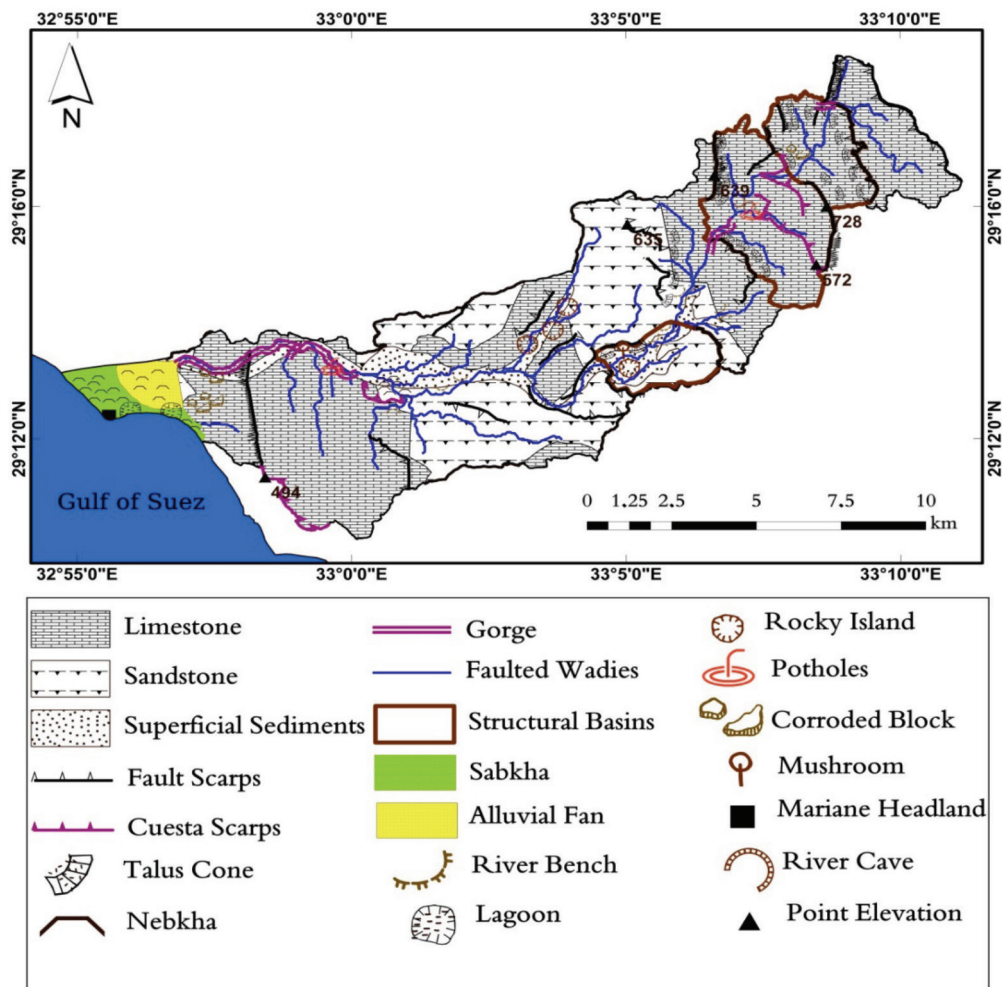


Fig. 11: Geomorphological map of the study area.

Data source: Geological and topographic map, SRTM, aerial images (Esri), and fieldwork.

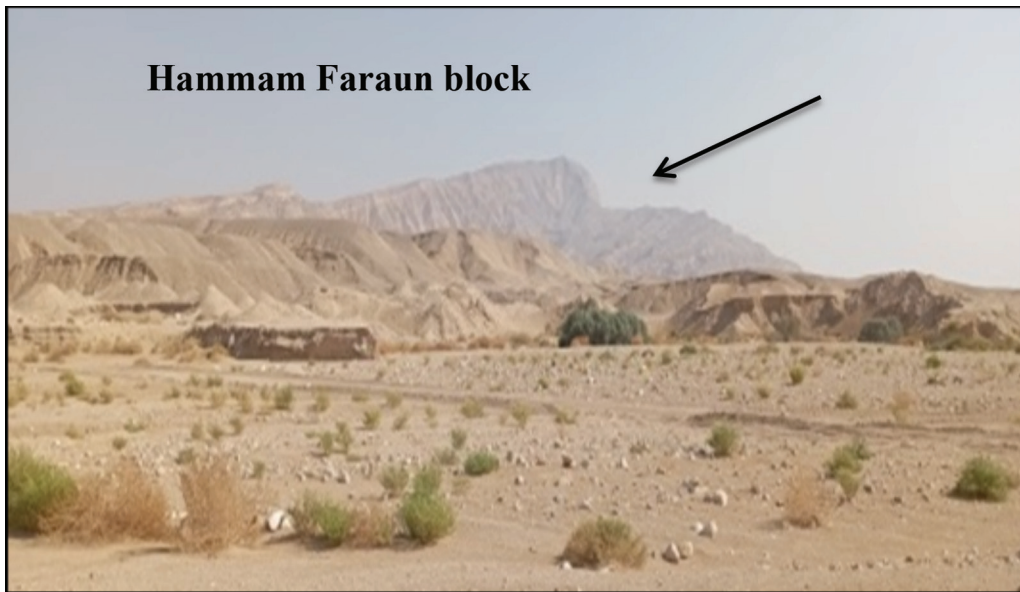


Fig. 12: The Fault Scarp of the Hammam Faraun block.



Fig. 13: The Cuesta scarp in Wadi Al-Darirah.

4.2.2. Structural Basins

A structural basin is a concave that is liable to the surrounding structural processes, and, therefore, it is highly affected by changes in these processes (Buiter, Adrian, 2003). It is a low basin that is situated between the surrounding fault scarps, which were formed by the faults extending in opposite directions

(Attalla, 2009).

The most important of these basins the Upper Sector in Wadi Al-Darirah, which extends to 7.4 km² and covers 5.8% of the study area. It is bounded on the east by the scarp of the Al-Darirah (Fig.14) and on the northwest by the scarp of the Heyala a long 885 m in the study area.

The scarp of the Heyala consists of chalky limestone and marl limestone rocks (Sidr - Isna). It is affected by the water streams, in addition to the formation of the talus cone in its Piedmont (Fig.15). The structural basin is bounded by the cuesta scarps in the west, which are Al-Darairah and Abu Al- Lasf .



Fig.14: The Structural Basin in wadi Al-Darirah.



Fig.15: The Heyala scarp.

4.2.3. *Faulted Wadies*

A Faulted Wadi is a valley whose streams run along fault lines (Zhang, et al., 2004). By integrating the results of analyzing geological maps into the hydrological analysis of the drainage networks in the basins of the study area, it was found that the main channels of the drainage basins are affected and directed by the

displacements of the faults. It is represented in the fourth, fifth, and sixth grades, with total real lengths of 106 km (Fig.11).

4.2.4. *Gorges*

Gorges form in areas of geological weakness. It is narrow extensions with slope sides. It is formed due to the tectonic processes and gully denudation (Torab, 2011).

It was founded in the lower sectors of the main Wadies in the study area. The most important of these gorges is the lower-sector gorge in Wadi Wasit (Fig.16: a). It was formed due to the exposure of the lower sector to tectonic processes. These processes consequently resulted in

1) the lifting of the Hammam Faraun block, 2) the change of the level of the base of the Wadi after its stagnation in the central sector of the study area (the Thal-Wasit concave fold), 3) restore stream activity due to the continuation of the gully denudation.

The gorge consists of dolomitic limestone rocks and Chert (Samalut Formation). Many geomorphological landforms in these resulted from the solution processes such as undercutting (Fig.16: b) and potholes in the lower sector of its Hanging Wadi.(Fig.16. c).

5-Conclusion

This study aims to determine the tectonic geomorphological landforms in Wadi Wasit in the Sinai Peninsula. It depended on Geological maps, Topographical maps, DEM (SRTM), Arial image (Esri), Global climate databases, and fieldwork. The data were processed and analyzed by using ArcGIS 10.5. Wadi Wasit consists of limestones, sandy rocks, and surface sediments. Its geomorphological landforms

were affected by tectonic processes during its geological development. The most important of these processes are flouting and folding. The tectonic geomorphological landforms in Wadi Wasit are Escarpments, Structural Basins, Faulted Wadies, and Gorges. There are climate geomorphological processes in the study area such as Gully Denudation, Vertical Erosion, Block Separation, Rock Shattering, Exfoliation, and Solution. This study showed a methodology for processing geological, topographical, hydrological, and climatic data. It is useful for planning and development.

6-References

- * Abu Al-Yazid, S. M., (2016). *Assessment of flood hazards in some basins east of the Gulf of Suez: Hydrogeomorphological study using hydrological models and remote sensing (PhD thesis)*. Faculty of Arts, Alexandria.
- *Al-Awadi, H. A. A., (1993). *The eastern coast region of the Gulf of Suez. A geomorphological study (PhD thesis)*. Faculty of Arts, Alexandria.
- *Al-Naggar, G. M., (2003). *Geomorphology of the Markha Plain, south west Sinai, Egypt. A study applying with special reference to remote sensing and GIS techniques (PhD thesis)*. Faculty of Arts, Alexandria.
- *Al-Rashidi, O. A., (1994). *Gharandal Basin*

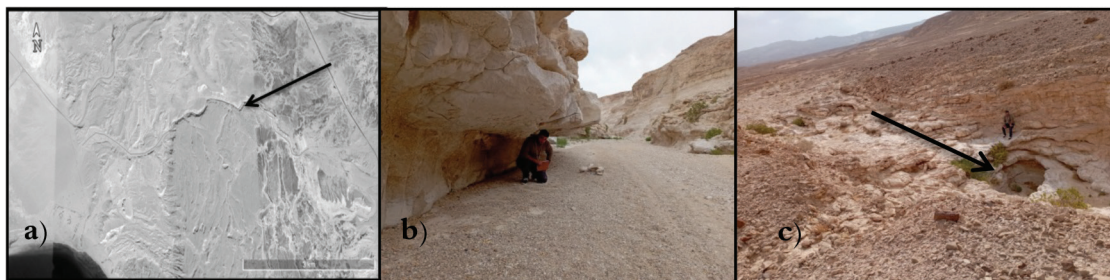


Fig.16: Morphology of the lower sector gorge in wadi Wasit.

- a) It has a length of 6,5 km, a mean width of 9,5 m, and River Meanders of 9.
- b) It has an elevation of 1,30 m and a deep of 1,50 m.
- c) It has a mean width of 3 m and a slop of (70 -90°).

Data source: POWER and ERA5.

"*Geomorphological Study*" (Master's Thesis). Faculty of Arts, Ain Shams.

* Al-Rifai et al., (Editing) (1998). *Geological Encyclopedia*. Kuwait: Kuwait Foundation for the Advancement of Sciences.

* Atallah, M. K., (2009). *Geology Basics*. Amman: Al Masirah for Publishing and Distribution.

* Ball, J., (1916). *The geography and geology of west-central Sinai*. Cairo, Egypt: Government Press.

* Buiter, S. J., Adrian, P., O., (2003). *Numerical models of the inversion of half-graben basins*. *Tectonics*, (22), 1-11.

* Chandler, W. S., Stackhouse J, P. W., Barnett, A. J., Hoell, J. M., Westberg, D. J., and Ross, A. I. (2015). Enhancing the NASA prediction of worldwide energy resource web data delivery system with geographic information system (GIS) capabilities No. NF 1676L-20865.

* Deshmane, M. K. S., Yadav, M. A. A., Ingawale, M. S. M., and Kamble, M. A. S., (2020). Wind data Estimation of Kolhapur district using Improved Hybrid Optimization by Genetic Algorithms (IHOGA) and NASA Prediction of Worldwide Energy Resources (NASA Power). *International Research Journal of Engineering and Technology (IRJET)*. 7(3), 2530-2538.

* Fabricius, I. L., (2007). Chalk: composition, diagenesis and physical properties. *Bulletin of the Geological Society of Denmark*, (55), 97-128.

* Ghallab, M. A. A. F., (2006). *Mount Hammam Pharaoh area between Wadi Abu Muhairiq and Thebes, the eastern coast of the Gulf of Suez "geomorphological study"* (Master's thesis). Faculty of Arts, Alexandria.

* Hassan, I. M. M., (2007). *Geomorphology*

of Alluvial fans in the eastern coast of the Gulf of Suez (master's thesis). Faculty of Arts, Alexandria

* Ismail, M. M. A., (2017). *Geomorphology of the bays on the eastern coast of the Gulf of Suez* (Master's Thesis). Faculty of Arts, Alexandria.

* Mareign, M. A., Mekonen, D. T., (2022) Estimating and mapping woodland biomass and carbon using Landsat 8 vegetation index: A case study in Dirmaga Watershed, Ethiopia. *Computational Ecology and Software*. 12(2), 67-79.

* Mashadi, H. K. I., (2005). *Geomorphological Hazards on the Eastern Side of Suez Gulf between Wadi Lahata in the North and Wadi El - Khashby in the South* (Master's Thesis). Faculty of Arts, El-Minya.

* Moustafa, A. R., (1996). Structural setting and tectonic evolution of the northern Hammam Faraun Block (Wadi Wasit-Wadi Wardan area), eastern side of the Suez rift. *Kuwait Journal of Science and Engineering*, (23), 105-131.

Moustafa, A. R., Abdeen, M. M., (1992). Structural setting of the Hammam Faraun block, eastern side of the Suez rift. *Journal University of Kuwait science*, (19), 291-291.

* Musaed, H., El-Kenawy, A., and El-Alfy, M. (2022). Morphometric, Meteorological, and Hydrologic Characteristics Integration for Rainwater Harvesting Potential Assessment in Southeast Beni Suef (Egypt). *Sustainability*, 14(21), 14183.

* Puri, P., Puri, V., (2022). The "First climate change famine" from 2017–2022-An analysis of the economics and geography of great SUD drought of Madagascar (1901–2021). *ACADEMICIA: An International Multidisciplinary Research Journal*, 12(3), 100-113.

* Qaqa, A. M. A., (2010). *The mountain slopes over the eastern side of the Gulf of Suez between the Ras Gulf of Suez and Ras Abu Zenima* (master's thesis). Faculty of Arts, Alexandria.

* Rockett, P., (2021). *Phenotypic and Genetic Analyses of Heat Tolerance in Holsteins using NASA Prediction of Worldwide Energy Resources (POWER) Weather Data*. Doctoral dissertation, University of Guelph.

*Różycka, M., Migoń, P., (2017). Tectonic geomorphology of the Sudetes (Central Europe)—a review and re-appraisal. *In Annales Societatis Geologorum Poloniae (Vol. 87)*, 275-300.

* Said, R., (1990). *The geology of Egypt*. Netherlands: Egyptian General Petroleum Corporation, Conoco Hurghada Incorporated and Repsol Exploracion, SA.

* Sando, R., Jaeger, K. L., Farmer, W. H., Barnhart, T. B., McShane, R. R., Welborn, T. L., and Shallcross, A., (2022). Predictions and drivers of sub-reach-scale annual streamflow permanence for the upper Missouri River basin: 1989–2018. *Journal of Hydrology*. Volume 17, 2-22.

* Shelby, M. S., (2013). *Geomorphological forms resulting from marine erosion on the eastern side of the Gulf of Suez between the Ras Al- Knais in the south and Ras Mosalh in the north using geographic information systems* (PhD thesis). Faculty of Arts, Banha.

* Smith, V., Warny, S., Jarzen, D. M., Demchuk, T., Vajda, V., and Gulick, S. P., (2020). Paleocene–Eocene palynomorphs from the Chicxulub impact crater, Mexico. Part 2: angiosperm pollen. *Palynology*, 44(3), 489-519.

* Stewart, I. S., Hancock, P. L., (1990). *What is a fault scarp?*. Episodes Journal of International

Geoscience, 13(4), 256-263.

Torab, M. M., (Editor) (2011). *Geomorphological Encyclopedia*, Alexandria.

*Torab, M., (2022). Geomorphology of the Al-Umrani paleo-karst cave (southeastern Egypt): its morphological determinants and links to the Nile Quaternary terraces. *The Egyptian Journal of Environmental Change*.

* Zhang, K., Liu, K., and Yang, J., (2004). Asymmetrical valleys created by the geomorphic response of rivers to strike-slip fault. *Quaternary Research*, 62(3), 310-315.

* Zhang, T., Stackhouse Jr, P. W., Chandler, W., Hoell, J. M., Westberg, D., and Whitlock, C. H. (2010). A global assessment of solar energy resources: NASA's Prediction of Worldwide Energy Resources (POWER) project. *In AGU Fall Meeting Abstracts*. Vol. 2010, U23A-0017.

* Zovoili, E., Konstantinidi, E., and Koukouvelas, I. K. (2004). Tectonic geomorphology of escarpments: The cases of kompotades and vea anchialos faults. *Bulletin of the Geological Society of Greece*, 36(4), 1716-1725.

